

# Quasinormal ringing of Kerr black holes.

## II. Excitation by particles falling radially with arbitrary energy

Zhongyang Zhang,<sup>1</sup> Emanuele Berti,<sup>1,2</sup> and Vitor Cardoso<sup>3,1,4</sup>

<sup>1</sup>*Department of Physics and Astronomy, The University of Mississippi, University, MS 38677, USA*

<sup>2</sup>*California Institute of Technology, Pasadena, CA 91109, USA*

<sup>3</sup>*CENTRA, Departamento de Física, Instituto Superior Técnico,*

*Universidade Técnica de Lisboa - UTL, Av. Rovisco Pais 1, 1049 Lisboa, Portugal*

<sup>4</sup>*Perimeter Institute for Theoretical Physics Waterloo, Ontario N2J 2W9, Canada*

The analytical understanding of quasinormal mode ringing requires an accurate knowledge of the Green’s function describing the response of the black hole to external perturbations. We carry out a comprehensive study of quasinormal mode excitation for Kerr black holes. Relying on the formalism developed by Mano, Suzuki and Takasugi, we improve and extend previous calculations of the quasinormal mode residues in the complex frequency plane (“excitation factors  $B_q$ ”). Using these results we compute the “excitation coefficients”  $C_q$  (essentially the mode amplitudes) in the special case where the source of the perturbations is a particle falling into the black hole along the symmetry axis. We compare this calculation with numerical integrations of the perturbation equations, and we show quantitatively how the addition of higher overtones improves the agreement with the numerical waveforms. Our results should find applications in models of the ringdown stage and in the construction of semianalytical template banks for gravitational-wave detectors, especially for binaries with large mass ratios and/or fast-spinning black holes.

### I. INTRODUCTION

Distorted black holes (BHs) emit gravitational radiation. A spectral decomposition of the perturbation response of the Schwarzschild [1] and Kerr [2] geometries using Green’s function techniques shows that a discrete sum of quasinormal modes (QNMs) – damped oscillations whose frequencies and damping times depend only on the BH mass and angular momentum – will dominate the response at all but very early and very late times. Because of the qualitative similarity with a ringing bell, this intermediate stage is known as “ringdown” in the gravitational-wave literature [3–5].

Numerical simulations show that binary BH mergers in general relativity inevitably result in the formation of a distorted rotating remnant, which radiates ringdown waves while settling down into a stationary (Kerr) solution of the Einstein equations in vacuum. Despite the great advances in binary BH simulations in four [6–8] and higher dimensions [9], the excitation of the QNMs of the remnant BH resulting from a merger is still poorly understood. Perturbative techniques are especially valuable to understand ringdown excitation in situations that pose a particular challenge to numerical simulations, namely:

1) *Large mass-ratio binaries.* One of the frontiers in numerical simulations of BH mergers are quasicircular binaries with large mass ratios. Progress in this direction has been slow but steady, both in the quasicircular case – where initial record mass ratios  $q = m_1/m_2 = 10$  [10] have been broken using “hybrid” techniques [11, 12] – and in the head-on case, where simulations with  $q = 100$  have recently been performed using different approaches [13, 14]. In this regime, perturbation theory is crucial to validate and/or optimize numerical simulations.

2) *Large spins.* Numerical simulations of BH binaries are usually carried out using either the Baumgarte-Shapiro-

Sasaki-Nakamura (BSSN) formulation of the Einstein equations and a finite-difference scheme, or using the harmonic formulation and spectral methods. The first class of simulations is limited to dimensionless spins  $a/M = J/M^2 \lesssim 0.93$ , because this is the maximum spin that can be achieved with puncture initial data [15]. Initial data with spins as large as  $a/M \sim 0.97$  can be constructed [16] and have been evolved using spectral codes [17, 18]. These simulations present a significant challenge for modeling efforts using effective-one-body techniques when one considers binaries with aligned spins  $a/M \gtrsim 0.7$  [19]. Models of the late merger and ringdown phase can be significantly improved by using first-principle calculations in BH perturbation theory, rather than a phenomenological matching of inspiral waveforms with QNM superpositions of largely arbitrary amplitudes and starting times.

3) *Higher dimensions.* Numerical simulations in higher dimensions are very challenging, and simple calculations in BH perturbation theory can give insight into the results of the simulations. For example, the qualitative behavior of the energy and linear momentum radiated by particles falling into higher-dimensional Schwarzschild-Tangherlini BHs (predicted in [20, 21]) is in excellent agreement with the first numerical simulations in  $D = 5$  [22]: see e.g. [23, 24] for reviews.

First-principle calculations of QNM excitation in four space-time dimensions would be particularly beneficial in building semianalytical models of the merger/ringdown phase, to be used as matched-filtering templates in gravitational-wave searches. Here we carry out these calculations in four spacetime dimensions considering, for simplicity, head-on particle infalls into Schwarzschild and Kerr BHs. Our study improves and extends the results of [2].

### A. Excitation factors and excitation coefficients

The gravitational radiation from a perturbed Kerr BH is usually described in terms of the Weyl scalar  $\psi_4$  [25, 26], which can be decomposed in different multipolar components (say  $\psi_{lm}$ ) by using spin-weighted spheroidal harmonics with angular indices  $(l, m)$  (see e.g. [27]). In the ringdown stage, each  $\psi_{lm}$  can be expressed as a sum of complex exponentials: schematically,

$$\psi_{lm} \sim \sum_{n=0}^{\infty} C_{lmn} \exp[-i\omega_{lmn}(t - r_*)], \quad (1)$$

where the frequencies  $\omega_{lmn}$  are complex,  $t$  denotes time as measured by an observer at infinity,  $r_*$  is a radial ‘‘tortoise’’ coordinate, and the index  $n$  (‘‘overtone index’’) sorts the modes by increasing imaginary part ( $n = 0$  corresponding to the smallest imaginary part and to the longest damping time). To simplify the notation, we will sometimes replace the indices  $(l, m, n)$  by a collective index  $q$ .

The problem of extracting the QNM contribution to a generic signal was first studied in detail by Leaver [1]. The complex amplitudes  $C_q$  of each complex exponential, also called ‘‘excitation coefficients’’, depend on the source of the perturbation (see e.g. [28–30]). The excitation coefficients can be factorized into the product  $C_q = B_q I_q$  of a source-independent ‘‘excitation factor’’  $B_q$  and of a source-dependent integral  $I_q$ . The integral  $I_q$  is in general divergent, but it can be regularized, yielding a finite answer in agreement with other perturbative calculations [1, 31–33].

To illustrate the origin of this factorization, consider the following prototypical ODE governing arbitrary perturbations around a BH. The perturbation is characterized by a wave function  $\Psi$  with source  $Q$  (representing for example the perturbation due to infalling matter):

$$\frac{\partial^2}{\partial r_*^2} \Psi - \frac{\partial^2}{\partial t^2} \Psi - V \Psi = -Q(t), \quad (2)$$

where  $r_*$  is a radial ‘‘tortoise coordinate’’, and the potential  $V = V(r_*)$ . The wave function  $\Psi$  can describe curvature-related quantities in the formalism by Sasaki and Nakamura [34] and it is directly related to metric perturbations in the Regge-Wheeler/Zerilli formalism [35, 36].

The QNM contribution to the time-domain Green’s function  $G_Q$  reads

$$\Psi_Q(r_*, t) = \int_{-\infty}^{\infty} \int_{-\infty}^{\infty} G_Q(r_*, t|r'_*, t') Q(r'_*, t') dr'_* dt',$$

where (see e.g. [1])

$$\begin{aligned} G_Q(r_*, t|r'_*, t') &= \\ &= 2\text{Re} \left[ \sum_{q=0}^{\infty} B_q \psi_q(r_*) \psi_q(r'_*) e^{-i\omega_q(t-t'-r_*-r'_*)} \right]. \end{aligned} \quad (3)$$

The coefficients  $B_q$  are the (source-independent) *excitation factors*, and  $\psi_q(r)$  denotes solutions of the homogeneous equation normalized such that  $\psi_q(r) \rightarrow 1$  as  $r_* \rightarrow \infty$ . It is convenient to introduce also the source-dependent *excitation coefficients*  $C_q$ :

$$C_q = B_q I_q, \quad (4)$$

where

$$I_q \equiv \int_{-\infty}^{\infty} e^{i\omega_q r'_*} \psi_q(r'_*) q(r'_*, \omega) dr'_*, \quad (5)$$

and where the frequency-domain source term is

$$q(r'_*, \omega) = \int_{-\infty}^{\infty} e^{i\omega t'} Q(r'_*, t') dt'. \quad (6)$$

The calculation of the  $C_q$ ’s involves an integral in  $r_*$  from the horizon ( $r_* = -\infty$ ) out to spatial infinity ( $r_* = \infty$ ). The integral usually diverges at the horizon; one of the proposed methods to eliminate this divergence is discussed below in Section III C. With these definitions, the ringdown waveform can be written as:

$$\Psi(r_*, t) = 2\text{Re} \left[ \sum_{q=0}^{\infty} C_q \psi_q(r_*) e^{-i\omega_q(t-r_*)} \right]. \quad (7)$$

As  $r_* \rightarrow \infty$  we have  $\psi_q(r_*) \rightarrow 1$ , so that

$$\Psi_Q(r_* \rightarrow \infty, t) = 2\text{Re} \left[ \sum_{q=0}^{\infty} C_q e^{-i\omega_q(t-r_*)} \right]. \quad (8)$$

To summarize, the complex excitation factors  $B_q$  are a ‘‘universal’’ intrinsic property of the BH which describes the excitability of each mode, independently of the source of the excitation. On the other hand, the complex excitation coefficients  $C_q$  are related to the amplitude of each QNM in response to a *specific* source inducing the oscillations.

### B. Plan of the paper

In the first part of this paper (Section II) we compute a catalog of QNM excitation factors  $B_q$  for Kerr BHs using the formalism developed by Mano, Suzuki and Takasugi ([37, 38], henceforth MST). By using this technique we confirm and extend results obtained some years ago by two of us [2]. The main advantage of the MST method is that it does not require the (generally nontrivial) evaluation of Coulomb wave functions, which was instead necessary in [2]. This allows us to produce accurate tables of the  $B_q$ ’s for the modes that are most interesting in gravitational-wave detection (multipolar indices  $l \leq 7$  and overtone indices  $n = 0, \dots, 4$ ). These tables (and similar tables for perturbations of spin  $s = 0$  and  $s = 1$ ) will be made publicly available on a website, along with a MATHEMATICA notebook that can be adapted to generate further tables if necessary [39].

In the second part of the paper we compute the excitation coefficients  $C_q$  for a classic problem in perturbation theory: the calculation of the gravitational radiation emitted by particles falling into the BH. We generalize work carried out by Leaver more than 25 years ago [1] (see also [31]). Whereas Leaver considered only infalls from rest into a Schwarzschild BH, we present detailed comparisons between numerical waveforms and excitation coefficient calculations for particles falling with arbitrary energy into Schwarzschild BHs (Section III) and we also consider the case where the BH is rotating (Section IV). In Section V we summarize our findings and point out possible directions for future work. Appendix A gives details about the regularization of divergent integrals in both the Schwarzschild and Kerr cases. In the whole paper we use geometrical units ( $G = c = 1$ ).

## II. EXCITATION FACTORS IN THE MANO-SUZUKI-TAKASUGI FORMALISM

In this Section we present a detailed calculation of the excitation factors  $B_q$  for Kerr QNMs. We follow the MST formalism ([37]; see also [38, 40]) and we refer to the original papers for a more organic presentation of the material; our intention here is to give a practical guide to the calculation of the  $B_q$ 's within this formalism. The method is different from – but equivalent to – Leaver's method [1], that was used by two of us in [2]. The main advantage of the MST formalism over Leaver's method is that the MST formalism does not require any (cumbersome) *evaluation* of Coulomb wave functions, as in Leaver's original treatment, but only a *matching* of the Coulomb-series expansion near infinity to an expansion in terms of hypergeometric functions near the horizon, which is simpler to perform in practice.

We will compute the excitation factors in both the Teukolsky and Sasaki-Nakamura formalisms (see [2] for a discussion). To begin with, let us define some quantities that will be used below:

$$\begin{aligned} r_{\pm} &= M \pm \sqrt{M^2 - a^2}, \quad \kappa = \sqrt{1 - j^2}, \\ x &= \frac{\omega(r_+ - r)}{\epsilon\kappa}, \quad \tau = \frac{\epsilon - am/M}{\kappa}, \quad \epsilon_{\pm} = \frac{\epsilon \pm \tau}{2}. \end{aligned} \quad (9)$$

From now on we follow Leaver's conventions and set  $2M = 1$  (where  $M$  is the BH mass). In these units, the parameter  $a \in [0, 1/2]$ . In order to make contact with the more usual  $M = 1$  units, we find it convenient to introduce a second dimensionless spin parameter  $j \equiv 2a \in [0, 1]$ . For reference, intermediate results of our calculations for a specific value of the spin ( $a = 0.4$ , or  $j = 0.8$ ) are given in Table I. In the remainder of this Section we will define and compute the quantities listed in this Table.

### A. Computing $\omega_q$ and $A_{lm}$

In the Teukolsky formalism, the perturbations of a Kerr BH are described by the Newman-Penrose scalar  $\psi_4$ , which is related to solutions  $\phi$  of the Teukolsky equation by  $\phi \equiv \rho^{-4}\psi_4$ , where  $\rho = (r - ia \cos \theta)^{-1}$ . By expanding in Fourier components

$$\rho^{-4}\psi_4 = \frac{1}{2\pi} \sum_{l=|s|}^{\infty} \sum_{m=-l}^l \int e^{-i\omega t + im\varphi} S_{lm\omega}(\theta) R_{lm\omega}(r) d\omega$$

and performing a separation of variables, one finds that the radial function  $R_{lm\omega}$  and the angular function  $S_{lm}$  must satisfy the following equations:

$$\Delta \frac{d^2 R_{lm\omega}}{dr^2} + (s+1)(2r-1) \frac{dR_{lm\omega}}{dr} + V(r) R_{lm\omega} = T_{lm\omega}, \quad (10)$$

$$\frac{d}{du} \left( (1-u^2) \frac{dS_{lm}}{du} \right) + \left[ a^2 \omega^2 u^2 - 2a\omega su + s + A_{lm} - \frac{(m+su)^2}{1-u^2} \right] S_{lm} = 0, \quad (11)$$

where  $u = \cos \theta$  and  $T_{lm\omega}$  is the Fourier transform of the stress-energy tensor after separation of the angular dependence. The potential  $V(r)$  is given by

$$\begin{aligned} V(r) &= \{ (r^2 + a^2)^2 \omega^2 - 2am\omega r + a^2 m^2 \\ &\quad + is[am(2r-1) - \omega(r^2 - a^2)] \} \Delta^{-1} \\ &\quad + 2is\omega r - a^2 \omega^2 - A_{lm}, \end{aligned} \quad (12)$$

where  $A_{lm}$  is the angular separation constant corresponding to the angular eigenfunctions  $S_{lm}$  (known as ‘‘spin-weighted spheroidal harmonics’’). The eigenfrequency  $\omega_{lmn} = \omega_q$  and the angular eigenvalue  $A_{lm}$  are determined by imposing QNM boundary conditions on the

radial equation (10) and regularity conditions on the angular equation (11): see e.g. [5]. The radial and angular equations are solved via a series solution whose coefficients  $b_n^r$  and  $b_n^\theta$  satisfy three-term recursion relations of the form

$$\begin{aligned} \alpha_0^\theta b_1^{(r,\theta)} + \beta_0^{(r,\theta)} b_0^{(r,\theta)} &= 0, \\ \alpha_n^{(r,\theta)} b_{n+1}^{(r,\theta)} + \beta_n^{(r,\theta)} b_n^{(r,\theta)} + \gamma_n^{(r,\theta)} b_{n-1}^{(r,\theta)} &= 0, \end{aligned} \quad (13)$$

where the superscript ( $r$  or  $\theta$ ) denotes association with the radial or angular equation, and the coefficients of the three-term recursion relations can be found in [41].

	$s = -2, l = m = 2$	$s = -1, l = m = 1$	$s = 0, l = m = 2$
$\omega_q$	1.172034 - 0.151259i	0.701679 - 0.152621i	1.41365 - 0.163041i
$A_{lm}$	2.585294 + 0.205297i	1.67659 + 0.0810074i	5.95475 + 0.0106275i
$\nu$	-1.743843 - 0.701583i	-1.69028 - 0.320182i	-1.8012 - 0.0481726i
$a_4^\nu$	$-1.32616 \times 10^{-3} + 1.43416 \times 10^{-3}i$	$-4.04792 \times 10^{-3} + 3.01211 \times 10^{-3}i$	$-0.229461 - 0.0295086i$
$a_{-4}^\nu$	$-4.52814 \times 10^{-3} - 2.12986 \times 10^{-2}i$	$8.02490 \times 10^{-5} - 2.25538 \times 10^{-4}i$	$1.47272 \times 10^{-3} + 3.40832 \times 10^{-4}i$
$K_\nu$	$1.06144 \times 10^{-3} + 7.43631 \times 10^{-4}i$	$-0.0812872 + 0.0682523i$	$-12.0419 + 1.20138i$
$K_{-\nu-1}$	$-8.19837 \times 10^{-2} - 9.20267 \times 10^{-1}i$	$1.55992 + 1.23780i$	$18.6581 + 3.85088i$
$B_{lm\omega}^{\text{inc}}$	$-2.80111 \times 10^{-16} + 3.11473 \times 10^{-16}i$	$-4.51443 \times 10^{-15} - 2.05141 \times 10^{-15}i$	$6.08313 \times 10^{-14} + 1.91604 \times 10^{-14}i$
$B_{lm\omega}^{\text{ref}}$	3.16122 + 1.25413i	1.59262 - 0.363221i	1.27738 + 0.760771i
$B_{lm\omega}^{\text{trans}}$	15.4151 + 11.0126i	3.32227 + 0.409647i	0.496587 + 1.24305i
$\alpha_q^T$	0.114759 - 0.241821i	-1.25046 - 1.01565i	-0.154117 - 3.58899i
$B_q^T$	-0.240807 + 0.150102i	-0.153477 - 0.144681i	-0.0955564 + 0.0516867i
$B_q^{\text{SN}}$	-0.0911231 + 0.0613455i	-0.0298959 - 0.119248i	-0.0955564 + 0.0516867i

TABLE I. Some intermediate quantities necessary to compute the excitation factors for the fundamental mode ( $n = 0$ ) of a Kerr BH with  $a = 0.4$  (or  $j = 0.8$ ). The three columns refer to gravitational ( $s = -2$ ) perturbations with  $l = m = 2$ , electromagnetic ( $s = -1$ ) perturbations with  $l = m = 1$ , and scalar ( $s = 0$ ) perturbations with  $l = m = 2$ .

By the principle of minimal solutions, the convergence of the series obtained via the three-term recursion relations is guaranteed by two continued fraction relations (one coming from the radial series expansion, the other from the angular series expansion) of the form

$$\beta_0^\theta = \frac{\alpha_0^\theta \gamma_1^\theta}{\beta_1^\theta - \frac{\alpha_1^\theta \gamma_2^\theta}{\beta_2^\theta - \dots}}, \quad (14)$$

$$\beta_0^r = \frac{\alpha_0^r \gamma_1^r}{\beta_1^r - \frac{\alpha_1^r \gamma_2^r}{\beta_2^r - \dots}}. \quad (15)$$

or by any of their inversions, which are analytically – but not numerically – equivalent [41].

We now have two complex equations, (14) and (15), in two complex unknowns,  $\omega_q$  and  $A_{lm}$ . By solving these equations numerically we find the eigenvalues listed in the first two rows of Table I. Numerical practice shows that the  $q$ th inversion index for the radial equation is best suited for numerical searches of the  $q$ th overtone  $\omega_q$ . Numerical experimentation (and analytical arguments [27]) show that the optimal inversion number to find the angular eigenvalue with the correct limit as  $a \rightarrow 0$ , i.e.

$$A_{lm} \rightarrow l(l+1) - s(s+1), \quad (16)$$

is equal to  $l - \max(|m|, |s|)$ .

### B. Angular momentum parameter $\nu$ and matching function $K_\nu$

The basic idea of the MST method is to (1) find a first independent solution of the radial equation  $R_0^\nu$  in terms of a series of hypergeometric functions (which does not converge at spatial infinity) with expansion coefficients proportional to  $a_n^\nu$ , cf. Eq. (2.21) of [37]; (2) consider

Leaver’s construction of a series of Coulomb wave functions  $R_C^\nu$  that is valid near infinity; (3) notice that the two solutions are identical modulo a  $\nu$ -dependent constant, i.e.

$$R_0^\nu = K_\nu R_C^\nu. \quad (17)$$

The expansion coefficients  $a_n^\nu$  and the matching condition depend on an “angular momentum” parameter  $\nu$  which appears in the three-term recurrence relation

$$\alpha_n^\nu a_{n+1}^\nu + \beta_n^\nu a_n^\nu + \gamma_n^\nu a_{n-1}^\nu = 0, \quad (18)$$

where

$$\begin{aligned} \alpha_n^\nu &= \frac{i\epsilon\kappa(n+\nu+1+s+i\epsilon)(n+\nu+1+s-i\epsilon)}{(n+\nu+1)(2n+2\nu+3)(n+\nu+1+i\tau)^{-1}}, \\ \beta_n^\nu &= -\lambda - s(s+1) + (n+\nu)(n+\nu+1) + \epsilon^2, \\ &\quad + \epsilon(\epsilon - mq) + \frac{\epsilon(\epsilon - mq)(s^2 + \epsilon^2)}{(n+\nu)(n+\nu+1)}, \\ \gamma_n^\nu &= -\frac{i\epsilon\kappa(n+\nu-s+i\epsilon)(n+\nu-s-i\epsilon)}{(n+\nu)(2n+2\nu-1)(n+\nu-i\tau)^{-1}}. \end{aligned} \quad (19)$$

and  $\lambda$  is related to the separation constant  $A_{lm}$  by

$$\lambda = A_{lm} + (a\omega)^2 - 2am\omega. \quad (20)$$

The solution of the above recursion relation is “minimal” (i.e., the  $a_n^\nu$ ’s give rise to a convergent series) if

$$\beta_0^\nu = \frac{\alpha_{-1}^\nu \gamma_0^\nu}{\beta_{-1}^\nu - \frac{\alpha_{-2}^\nu \gamma_{-1}^\nu}{\beta_{-2}^\nu - \dots}} + \frac{\alpha_0^\nu \gamma_1^\nu}{\beta_1^\nu - \frac{\alpha_1^\nu \gamma_2^\nu}{\beta_2^\nu - \dots}}. \quad (21)$$

This condition is only satisfied by a discrete set of (complex) values of  $\nu$ . Different inversions of Eq. (21) yield different values of  $\nu$ : for example, we could consider the first inversion

$$\beta_1^\nu = \frac{\alpha_0^\nu \gamma_1^\nu}{\beta_0^\nu - \frac{\alpha_{-1}^\nu \gamma_0^\nu}{\beta_{-1}^\nu - \frac{\alpha_{-2}^\nu \gamma_{-1}^\nu}{\beta_{-2}^\nu - \dots}}} + \frac{\alpha_1^\nu \gamma_2^\nu}{\beta_2^\nu - \dots} \quad (22)$$

or even a sequence of “negative” inversions, such as

$$\beta_{-1}^\nu = \frac{\alpha_{-2}^\nu \gamma_{-1}^\nu}{\beta_{-2}^\nu - \dots} + \frac{\alpha_{-1}^\nu \gamma_0^\nu}{\beta_0^\nu - \frac{\alpha_0^\nu \gamma_1^\nu}{\beta_1^\nu - \frac{\alpha_1^\nu \gamma_2^\nu}{\beta_2^\nu - \dots}}}. \quad (23)$$

Inversions are useful also for the radial and angular continued fractions, but the numerical calculation of  $\nu$  is a little trickier: the numerical root  $\nu$  can be different for different inversions of the continued fraction, but this does not affect the physics of the problem. The reason is that the eigenvalues  $\nu$  have the following properties: (i)  $\nu$  has period equal to 1: if  $\nu$  is a solution,  $\nu \pm 1$  is also a solution; (ii) If  $\nu$  is a solution,  $-\nu$  is also a solution.

Given the eigenvalue  $\nu$  (as listed, e.g., in the third row of Table I), it is straightforward to build up the series coefficients  $a_n^\nu$  from the three-term recursion relation (18). If we choose the arbitrary normalization constant such that  $a_0^\nu = 1$ , we get (for example) the values of  $a_4^\nu$  and  $a_{-4}^\nu$  listed in rows four and five of Table I.

An important property of these coefficients is that  $a_{-n}^{-\nu-1} = a_n^\nu$ : this can be shown starting from the three-term recursion relation (18), and using Eqs. (19). Therefore we can denote them by  $a_n^\nu$  when they refer to  $K_\nu$ , and by  $a_{-n}^{-\nu-1}$  when they refer to  $K_{-\nu-1}$ .

As we will see below, to obtain the QNM excitation coefficients we must compute  $K_\nu$  and  $K_{-\nu-1}$ , given by Eq. (165) in [42]:

$$K_\nu = \frac{e^{i\epsilon\kappa} (2\epsilon\kappa)^{s-\nu-p} 2^{-s} i^p \Gamma(1-s-2i\epsilon_+) \Gamma(p+2\nu+2)}{\Gamma(p+\nu+1-s+i\epsilon) \Gamma(p+\nu+1+i\tau) \Gamma(p+\nu+1+s+i\epsilon)} \times \left( \sum_{n=-\infty}^p \frac{(-1)^n}{(p-n)! (p+2\nu+2)_n \frac{(\nu+1+s-i\epsilon)_n}{(\nu+1-s+i\epsilon)_n}} a_n^\nu \right)^{-1} \\ \times \left( \sum_{n=p}^{\infty} \frac{\Gamma(n+p+2\nu+1) \Gamma(n+\nu+1+s+i\epsilon) \Gamma(n+\nu+1+i\tau)}{(-1)^n (n-p)! \Gamma(n+\nu+1-s-i\epsilon) \Gamma(n+\nu+1-i\tau)} a_n^\nu \right), \quad (24)$$

where the notation  $(x)_n$  is a shorthand for the following function of  $x$ :

$$(x)_n \equiv \frac{\Gamma(x+n)}{\Gamma(x)}, \quad (25)$$

and  $p$  can be any integer. Both  $K_\nu$  and  $K_{-\nu-1}$  are independent of the choice of  $p$ ; indeed, this property can be used as a check of the calculation. Representative values of  $K_\nu$  and  $K_{-\nu-1}$  are listed in Table I.

### C. Amplitudes $B_{lm\omega}^{\text{inc}}$ , $B_{lm\omega}^{\text{ref}}$ and $B_{lm\omega}^{\text{trans}}$ in the Teukolsky formalism

According to Eqs. (167), (168) and (169) in [42], the ingoing-wave radial solution has the asymptotic behavior

$$R_{lm\omega}^{\text{in}} \rightarrow \begin{cases} B_{lm\omega}^{\text{trans}} \Delta^2 e^{-ikr^*} & \text{as } r \rightarrow r_+, \\ r^3 B_{lm\omega}^{\text{ref}} e^{i\omega r^*} + r^{-1} B_{lm\omega}^{\text{inc}} e^{-i\omega r^*} & \text{as } r \rightarrow +\infty, \end{cases} \quad (26)$$

where the amplitudes are defined as:

$$B_{lm\omega}^{\text{inc}} = \omega^{-1} \left( K_\nu - i e^{-i\pi\nu} \frac{\sin \pi(\nu-s+i\epsilon)}{\sin \pi(\nu+s-i\epsilon)} K_{-\nu-1} \right) A_+^\nu \\ \times e^{-i\epsilon \ln \epsilon}, \quad (27)$$

$$B_{lm\omega}^{\text{ref}} = \omega^{-1-2s} (K_\nu + i e^{i\pi\nu} K_{-\nu-1}) A_-^\nu e^{i\epsilon \ln \epsilon}, \quad (28)$$

$$B_{lm\omega}^{\text{trans}} = \left( \frac{\epsilon\kappa}{\omega} \right)^{2s} e^{i\epsilon_+ \ln \kappa} \sum_{n=-\infty}^{\infty} a_n^\nu, \quad (29)$$

and

$$A_+^\nu = e^{-(\pi/2)\epsilon} e^{(\pi/2)i(\nu+1-s)} 2^{-1+s-i\epsilon} \\ \times \frac{\Gamma(\nu+1-s+i\epsilon)}{\Gamma(\nu+1+s-i\epsilon)} \sum_{n=-\infty}^{\infty} a_n^\nu, \quad (30)$$

$$A_-^\nu = e^{-(\pi/2)\epsilon} e^{-(\pi/2)i(\nu+1+s)} 2^{-1-s+i\epsilon} \\ \times \sum_{n=-\infty}^{\infty} (-1)^n \frac{(\nu+1+s-i\epsilon)_n}{(\nu+1-s+i\epsilon)_n} a_n^\nu. \quad (31)$$

The QNM boundary conditions require that  $B_{lm\omega}^{\text{inc}}$  must vanish at the QNM frequencies  $\omega_q$ . Table I shows that this indeed happens within an accuracy very close to machine precision. The table also lists reference values for  $B_{lm\omega}^{\text{ref}}$  and  $B_{lm\omega}^{\text{trans}}$ .

### D. $\alpha_q^{\text{T}}$ in the Teukolsky formalism

The excitation factors (in the Teukolsky formalism) are defined as

$$B_q^{\text{T}} = -\frac{A_{\text{out}}^{\text{T}}(\omega_q)}{2i\omega_q \alpha_q^{\text{T}}}. \quad (32)$$

Here

$$\alpha_q^{\text{T}} \equiv i \left( \frac{dA_{\text{in}}^{\text{T}}}{d\omega} \right)_{\omega_q}, \quad (33)$$

and furthermore

$$A_{\text{in}}^{\text{T}} \equiv \frac{B_{lm\omega}^{\text{inc}}}{B_{lm\omega}^{\text{trans}}}, \quad A_{\text{out}}^{\text{T}} \equiv \frac{B_{lm\omega}^{\text{ref}}}{B_{lm\omega}^{\text{trans}}}. \quad (34)$$



Note that we can divide both  $B_{lm\omega}^{\text{inc}}$  and  $B_{lm\omega}^{\text{ref}}$  by some arbitrary function  $G(\omega)$  without affecting the excitation factors  $B_q^{\text{T}}$ . This is because  $B_{lm\omega}^{\text{inc}}$  must vanish at the QNM frequencies  $\omega_q$ , so  $G(\omega)$  is just an arbitrary rescaling (or normalization) factor. The proof is trivial:

$$B_q^{\text{T}} \propto \left( \frac{B_{lm\omega}^{\text{ref}}}{dB_{lm\omega}^{\text{inc}}/d\omega} \right)_{\omega_q} = \left( \frac{B_{lm\omega}^{\text{ref}}/G}{d[B_{lm\omega}^{\text{inc}}/G]/d\omega} \right)_{\omega_q} \quad (35)$$

The simplest choice would be to set  $G = 1$ , but in order to reproduce all of the values listed in Leaver's Table I [1], especially  $\alpha_q^{\text{SN}}$  and  $A_{\text{out}}^{\text{SN}}$ , we choose a normalization factor

$$G = B_{lm\omega}^{\text{trans}}. \quad (36)$$

To get  $\alpha_q^{\text{T}}$  we must compute the derivative of  $A_{\text{in}}^{\text{T}}$  with respect to  $\omega$ . We first compute  $A_{\text{in}}^{\text{T}}$  at the QNM frequency  $\omega_q$ ,  $A_{\text{in}}^{\text{T}}(\omega_q)$ . Then we consider a new frequency  $\omega_q + \delta$ , and we repeat the calculation described above to get  $A_{\text{in}}^{\text{T}}(\omega_q + \delta)$ ; note in particular that when we repeat the first step (as described in Section II A) we use the angular continued fraction to obtain a "new" angular constant, evaluated at  $\omega_q + \delta$ . Finally we can compute the derivative by finite differencing:

$$\alpha_q^{\text{T}} = i \frac{A_{\text{in}}^{\text{T}}(\omega_q + \delta) - A_{\text{in}}^{\text{T}}(\omega_q)}{\delta}. \quad (37)$$

In our calculation we set  $\delta = 10^{-7}$  (i.e. we differentiate along the real axis); as a check of our finite-differencing procedure we also repeat the calculation with  $\delta = 10^{-7}i$  (i.e., differentiating along the pure-imaginary axis). The two results usually agree to better than one part in  $10^6$ .

### E. Excitation factors in the Teukolsky ( $B_q^{\text{T}}$ ) and Sasaki-Nakamura ( $B_q^{\text{SN}}$ ) formalisms

The excitation factors in the Teukolsky formalism were defined in Eq. (32). It turns out that for many practical purposes, including the calculation of radiation from infalling point particles that will be presented later on in this paper, it is more convenient to use the Sasaki-Nakamura wave function  $X$ , related to Teukolsky's by

$$X = \frac{\sqrt{r^2 + a^2}}{\Delta} \left( \alpha(r)R + \frac{\beta(r)}{\Delta}R' \right), \quad (38)$$

where the prime stands for a derivative with respect to  $r$ . Specializing to the case presented in Appendix B of Sasaki and Nakamura [34] [i.e.,  $f = h = 1$  and  $g = (r^2 + a^2)/r^2$ ], the functions  $\alpha$  and  $\beta$  are, respectively:

$$\alpha = -\frac{iK}{\Delta^2}\beta + 3iK' + \lambda + \frac{6\Delta}{r^2}, \quad (39)$$

$$\beta = \Delta \left[ -2iK + \Delta' - 4\frac{\Delta}{r} \right]. \quad (40)$$

Here  $K = (r^2 + a^2)\omega - am$ ,  $\Delta = r^2 - 2Mr + a^2$  and  $\lambda$  was defined in Eq. (20). Then the Sasaki-Nakamura wave function  $X$  satisfies

$$\frac{d^2X}{dr_*^2} - \mathcal{F}\frac{dX}{dr_*} - \mathcal{U}X = \mathcal{S}, \quad (41)$$

where the tortoise coordinate is defined as  $\frac{dr}{dr_*} = \frac{r^2 + a^2}{\Delta}$ . The tortoise coordinate is defined up to an integration constant, which we fix once and for all by setting

$$r_* = r + \frac{2Mr_+}{r_+ - r_-} \log(r - r_+) - \frac{2Mr_-}{r_+ - r_-} \log(r - r_-). \quad (42)$$

The functions  $\mathcal{F}$  and  $\mathcal{U}$  are given by

$$\begin{aligned} \mathcal{F} &= \frac{\Delta}{r^2 + a^2}F, \quad F \equiv \frac{\gamma'}{\gamma}, \\ \gamma &\equiv \alpha \left( \alpha + \frac{\beta'}{\Delta} \right) - \frac{\beta}{\Delta} \left( \alpha' - \frac{\beta}{\Delta^2}V \right), \\ \mathcal{U} &= \frac{\Delta U}{(r^2 + a^2)^2} + G^2 + \frac{dG}{dr_*} - \frac{\Delta GF}{r^2 + a^2}, \\ G &\equiv -\frac{\Delta'}{r^2 + a^2} + \frac{r\Delta}{(r^2 + a^2)^2}, \\ \mathcal{U} &= -V + \frac{\Delta^2}{\beta} \left[ \left( (2\alpha + \frac{\beta'}{\Delta})' - \frac{\gamma'}{\gamma} \left( \alpha + \frac{\beta'}{\Delta} \right) \right) \right]. \end{aligned}$$

Note that our Teukolsky potential  $V$  differs by an overall minus sign from the potential used by Sasaki and Nakamura, and that

$$\lim_{r \rightarrow \infty} \gamma \equiv \gamma_\infty = \lambda(2 + \lambda) - 12iM\omega - 12a\omega(\omega a - m). \quad (43)$$

When  $a \rightarrow 0$  the Sasaki-Nakamura potential reduces, by construction, to the so-called Regge-Wheeler potential (cf. Section III below for more details). The asymptotic behavior of the Sasaki-Nakamura wave function is

$$X \sim A_{\text{trans}} e^{-ikr_*}, \quad r \rightarrow r_+, \quad (44)$$

$$X \sim A_{\text{in}} e^{-i\omega r_*} + A_{\text{out}} e^{i\omega r_*}, \quad r \rightarrow \infty. \quad (45)$$

where  $k = \omega - am/r_+$ , and the coefficients can be related to the corresponding Teukolsky coefficients by

$$A_{\text{in}}^{\text{T}} = -\frac{1}{4\omega^2} A_{\text{in}}, \quad (46)$$

$$A_{\text{out}}^{\text{T}} = -\frac{4\omega^2}{\lambda(\lambda + 2) - 6i\omega - 12a\omega(\omega a - m)} A_{\text{out}}, \quad (47)$$

and  $\lambda \equiv A_{lm} + (a\omega)^2 - 2am\omega$ . The normalization at the horizon is such that

$$\begin{aligned} A_{\text{trans}} &= r_+^{1/2} [(8 - 12i\omega - 4\omega^2)r_+^2 \\ &\quad + (12iam - 8 + 8am\omega + 6i\omega)r_+ \\ &\quad - 4a^2m^2 - 6iam + 2]. \end{aligned} \quad (48)$$

A change of wave function of the form

$$X = \exp \left[ \int \frac{\mathcal{F}}{2} dr_* \right] X_2 = X_2 \sqrt{\gamma} \quad (49)$$

eliminates the first derivative, yielding

$$\frac{d^2 X_2}{dr_*^2} + \left( \frac{\mathcal{F}'}{2} - \frac{\mathcal{F}^2}{4} - \mathcal{U} \right) X_2 = \mathcal{S} \exp \left[ - \int \frac{\mathcal{F}}{2} dr_* \right] = \frac{\mathcal{S}}{\sqrt{\gamma}}. \quad (50)$$

To get the excitation factors in the Sasaki-Nakamura formalism we only need the asymptotic relation between  $X$  and  $R$ , Eq. (47) (similar relations are presented in [2] for scalar and electromagnetic perturbations). Denoting scalar, electromagnetic and gravitational perturbations by the subscript 0,  $-1$  and  $-2$  respectively, and dropping the “ $q$ ” subscripts to simplify the notation, we have:

$$B_0^{\text{SN}} = B_0^{\text{T}}, \quad (51)$$

$$B_{-1}^{\text{SN}} = - \frac{2am\omega_q - A_{lm} - a^2\omega_q^2}{4\omega_q^2} B_{-1}^{\text{T}}, \quad (52)$$

$$B_{-2}^{\text{SN}} = \frac{\lambda(\lambda+2) - 6i\omega_q - 12a\omega_q(a\omega_q - m)}{16\omega_q^4} B_{-2}^{\text{T}}. \quad (53)$$

The results for  $a = 0.4$  ( $j = 0.8$ ) are listed in the last row of Table I. All of the  $B_q$ 's (for  $s = 0, -1, -2$ ) match the results of Paper I, but now the computation does not involve tricky evaluations of the Coulomb wave functions. This allows us to compute excitation factors for a larger range of spin values, and for a larger set of values of  $(l, m)$  and of the overtone number  $n$ . An extensive catalog of results for Kerr perturbations of spin  $s = 0, 1$  and  $2$ ,  $l = s, \dots, 7$  and  $n = 0, \dots, 3$  is provided online in the form of downloadable numerical tables [39].

### III. EXCITATION FACTORS AND EXCITATION COEFFICIENTS FOR SCHWARZSCHILD BLACK HOLES

#### A. Excitation factors for the Zerilli and Regge-Wheeler equations

Perturbations of rotating (Kerr) BHs are conveniently described using curvature-related quantities in the Newman-Penrose approach. As discussed in the previous section, this naturally leads to the definition of the excitation factors in either the Teukolsky or Sasaki-Nakamura formalism (the latter being more suitable to

numerical calculations, due to the short-range nature of the source term of the Sasaki-Nakamura equation).

For the Schwarzschild BH geometry, a (perhaps more physically transparent) direct metric perturbation treatment can be performed. The perturbations separate in two sectors depending on their behavior under parity: the axial (or odd) and polar (or even) sector. Odd-parity metric perturbations can be found from the Regge-Wheeler wave function  $\Psi^{(-)}$ , and even-parity perturbations lead to the Zerilli equation for a single wave function  $\Psi^{(+)}$ . In both cases the problem reduces to the solution of a wave equation of the form

$$\frac{\partial^2}{\partial r_*^2} \Psi^{(\pm)} - \frac{\partial^2}{\partial t^2} \Psi^{(\pm)} - V^{(\pm)} \Psi^{(\pm)} = -Q^{(\pm)}(t). \quad (54)$$

Defining  $\lambda = (l-1)(l+2)/2$ , the Zerilli potential reads

$$V^{(+)} = \left( \frac{r-1}{r} \right) \frac{8\lambda^2(\lambda+1)r^3 + 12\lambda^2r^2 + 18\lambda r + 9}{r^3(2\lambda r + 3)^2} \quad (55)$$

whereas the Regge-Wheeler potential reads

$$V^{(-)} = \frac{r-1}{r^3} \left[ l(l+1) - \frac{3}{r} \right]. \quad (56)$$

These equations can be solved in the frequency domain using the approach followed by Leaver [1] and summarized below. At the QNM frequencies, the Regge-Wheeler wave function, normalized such that  $\psi_q^{(-)}(r) \rightarrow 1$  as  $r \rightarrow \infty$ , reads:

$$\psi_q^{(-)}(r) = \left( 1 - \frac{1}{r} \right)^{-2i\omega_q} \left[ \sum_{n=0}^{\infty} a_n(\omega_q) \right]^{-1} \times \left[ \sum_{n=0}^{\infty} a_n(\omega_q) (1 - 1/r)^n \right], \quad (57)$$

where the coefficients  $a_n$  can be computed from a three-term recursion relation (cf. Appendix A in [1]). A simple relation between the homogeneous solutions of the Zerilli and Regge-Wheeler equation was found by Chandrasekhar [43] (see also Eqs. (102)-(104) in [1]). Using the Chandrasekhar transformation, we find that the Zerilli wave function  $\psi_q^{(+)}(r)$ , again normalized such that  $\psi_q^{(+)}(r) \rightarrow 1$  as  $r \rightarrow \infty$ , is

$$\psi_q^{(+)}(r) = \frac{(1-1/r)^{-2i\omega_q}}{\sum a_n} \sum_{n=0}^{\infty} \left[ \left( 1 + \frac{-6i\omega_q(2\lambda r + 3) + 9(r-1)}{r^2(2\lambda r + 3)[2\lambda(\lambda+1) + 3i\omega_q]} + \frac{3n}{r^2[2\lambda(\lambda+1) + 3i\omega_q]} \right) a_n \left( \frac{r-1}{r} \right)^n \right]. \quad (58)$$

As explained in Section IA, the QNM contribution to the time-domain Green's function reads

$$\Psi_Q^{(\pm)}(r_*, t) = \int_{-\infty}^{\infty} \int_{-\infty}^{\infty} G_Q^{(\pm)}(r_*, t | r'_*, t') Q^{(\pm)}(r'_*, t') dr'_* dt',$$

with

$$G_Q(r_*, t | r'_*, t') = 2\text{Re} \left[ \sum_{q=0}^{\infty} B_q^{(\pm)} \psi_q^{(\pm)}(r) \psi_q^{(\pm)}(r') e^{-i\omega_q(t-t'-r_*-r'_*)} \right] \quad (59)$$

$B_q^{(-)}$	$l = 2$	$l = 3$	$l = 4$	$l = 5$
$n = 0$	0.126902 + 0.0203152i	-0.0938898 - 0.0491928i	0.065348 + 0.0652391i	-0.0384465 - 0.0735239i
$n = 1$	0.0476826 - 0.223755i	-0.151135 + 0.269750i	0.261488 - 0.251524i	-0.363440 + 0.182660i
$n = 2$	-0.190284 + 0.0157486i	0.415029 + 0.141038i	-0.549217 - 0.435328i	0.534171 + 0.828615i
$n = 3$	0.0808676 + 0.0796126i	-0.0434028 - 0.412747i	-0.316921 + 0.837911i	1.08630 - 1.14858i
$B_q^{(+)}$	$l = 2$	$l = 3$	$l = 4$	$l = 5$
$n = 0$	0.120923 + 0.0706696i	-0.0889796 - 0.0611757i	0.0621266 + 0.069100i	-0.0364029 - 0.0748073i
$n = 1$	0.158645 - 0.253334i	-0.191928 + 0.264820i	0.279700 - 0.241825i	-0.371542 + 0.173592i
$n = 2$	-0.298933 - 0.0711341i	0.436786 + 0.204560i	-0.543211 - 0.478060i	0.517754 + 0.854935i
$n = 3$	0.113837 + 0.204137i	-0.000920468 - 0.476365i	-0.374502 + 0.859526i	1.13916 - 1.14048i

TABLE II. Odd- and even-parity excitation factors for  $l = 2, 3, 4, 5$ .

Because the Sasaki-Nakamura wave function reduces to the Regge-Wheeler wave function when  $a \rightarrow 0$ , the corresponding excitation factors are related by

$$B_q^{(-)} = B_{-2}^{\text{SN}}(a = 0). \quad (60)$$

The even-parity excitation factors  $B_q^{(+)}$  are related to the odd-parity excitation factors  $B_q^{(-)}$  by [1, 43]

$$B_q^{(+)} = B_q^{(-)} \frac{2\lambda(\lambda + 1) + 3i\omega_q}{2\lambda(\lambda + 1) - 3i\omega_q}. \quad (61)$$

Thus, one can compute excitation factors for both the Regge-Wheeler and Zerilli representations using the excitation factors computed in Section II.

For completeness, in Table II we list the axial ( $B_q^{(-)}$ ) and polar ( $B_q^{(+)}$ ) Schwarzschild excitation factors for the fundamental mode and for the first three overtones with  $l = 2, 3, 4, 5$ . From Table II we see that the absolute values of the excitation factors  $|B_q^{(\pm)}|$  for different overtone numbers  $n$  and fixed  $l$  are of comparable magnitude. Values of these coefficients up to  $l = 7$  can be computed using the data available at [39].

### B. Excitation coefficients for low- and high-energy particle infalls

We will now compute the source-dependent excitation coefficients  $C_q$  and compare them with actual waveforms for head-on infalls into Schwarzschild or Kerr BHs along the symmetry axis. This is a classic problem addressed via the Regge-Wheeler-Zerilli formalism for non-rotating BHs [44] and via the Sasaki-Nakamura formalism for Kerr BHs [34]. The original analysis was revisited by several authors, who considered particles falling with generic energy and from finite distance into Schwarzschild BHs, Kerr BHs, and higher-dimensional BHs [20, 21, 45–51]. In four dimensions, head-on collisions with large mass ratio have even become accessible to simulations in full numerical relativity [13, 14].

In general, the source-dependent excitation coefficients  $C_q^{(\pm)}$  are given by

$$C_q^{(\pm)} = B_q^{(\pm)} I_q^{(\pm)}, \quad (62)$$

where

$$I_q^{(\pm)} \equiv \int_1^\infty e^{i\omega_q r'} \psi_q^{(\pm)}(r') q^{(\pm)}(r', \omega) (r' - 1)^{i\omega_q - 1} r' dr', \quad (63)$$

and where  $q^{(\pm)}(r', \omega)$  denotes the frequency-domain source term. The calculation of the  $C_q^{(\pm)}$ 's involves an integral in  $r$  from the horizon ( $r = 1$ ) out to spatial infinity ( $r = \infty$ ). The integral usually diverges at the horizon, but this divergence can be eliminated, as discussed below.

For a four-dimensional Schwarzschild BH, radial infalls excite only even (polar) perturbations and the source term in the Fourier domain reads

$$q(r, \omega) = m_0 4\sqrt{2\pi} \sqrt{4l + 2} \frac{r - 1}{r(2\lambda r + 3)} \times \left[ \left( E^2 - 1 + \frac{1}{r} \right)^{-1/2} + \frac{4E\lambda}{i\omega(2\lambda r + 3)} \right] e^{i\omega T(r)}. \quad (64)$$

Here  $m_0$  is the rest mass,  $v_0$  is the speed of the particle at spatial infinity, and  $E = m_0/\sqrt{1 - v_0^2}$  is the (conserved) energy per unit mass of the infalling particle. For a particle falling from rest at infinity,  $E = 1$ ; for a particle falling ultrarelativistically,  $E \rightarrow \infty$ .

Since we work in perturbation theory, the amplitude of the radiation is proportional to  $m_0 E$ , and therefore it is useful to define the following rescaled quantities:

$$\tilde{C}_q = \frac{C_q^{(+)}}{m_0 E}, \quad \tilde{I}_q = \frac{I_q^{(+)}}{m_0 E}. \quad (65)$$

The function  $T(r)$  can be found by integrating the geodesic equations, namely

$$\frac{dT}{dr} = \frac{-rE}{(r - 1)\sqrt{E^2 - 1 + 1/r}}. \quad (66)$$



$E = 1$	$l = 2$	$l = 3$	$l = 4$	$l = 5$
$n = 0$	$-1.89425 - 0.906608i$	$-0.184934 - 0.231572i$	$-0.0178934 - 0.0566232i$	$0.000637468 - 0.0141310i$
$n = 1$	$-1.94463 - 0.521963i$	$-0.226114 - 0.187532i$	$-0.0288733 - 0.0511510i$	$-0.00228156 - 0.0137320i$
$n = 2$	$-2.02880 - 0.263614i$	$-0.266489 - 0.148876i$	$-0.0393956 - 0.0457755i$	$-0.00509258 - 0.0132048i$
$n = 3$	$-2.11182 - 0.115656i$	$-0.306561 - 0.116049i$	$-0.0496969 - 0.0405565i$	$-0.00784699 - 0.0125698i$
$E = 10$	$l = 2$	$l = 3$	$l = 4$	$l = 5$
$n = 0$	$-4.835573 + 0.874861i$	$-1.195880 + 0.0709923i$	$-0.449316 + 0.0101960i$	$-0.209552 + 0.00308825i$
$n = 1$	$-4.478522 + 0.683019i$	$-1.177329 + 0.0667378i$	$-0.446281 + 0.0112097i$	$-0.208268 + 0.00284264i$
$n = 2$	$-4.142391 + 0.502502i$	$-1.156297 + 0.0606733i$	$-0.443514 + 0.0110150i$	$-0.207551 + 0.00277215i$
$n = 3$	$-3.818084 + 0.354501i$	$-1.134168 + 0.0540593i$	$-0.440663 + 0.0104592i$	$-0.206954 + 0.00269149i$

TABLE III. Rescaled integrals  $\tilde{I}_q$  for  $l = 2, 3, 4, 5$  for particle with energy  $E = 1$  (top) and  $E = 10$  (bottom).

$E = 1$	$l = 2$	$l = 3$	$l = 4$	$l = 5$
$n = 0$	$-0.164989 - 0.243495i$	$0.00228872 + 0.0319187i$	$0.00280101 - 0.00475425i$	$-0.00108031 + 0.000466722i$
$n = 1$	$-0.440736 + 0.409836i$	$0.0930598 - 0.0238868i$	$-0.0204455 - 0.00732461i$	$0.00323146 + 0.00470595i$
$n = 2$	$0.587721 + 0.223120i$	$-0.0859447 - 0.119540i$	$-0.000483324 + 0.0436992i$	$0.00865255 - 0.0111907i$
$n = 3$	$-0.216793 - 0.444266i$	$-0.0549996 + 0.146142i$	$0.0534710 - 0.0275273i$	$-0.0232746 - 0.00536977i$
$E = 10$	$l = 2$	$l = 3$	$l = 4$	$l = 5$
$n = 0$	$-0.646559 - 0.235935i$	$0.110752 + 0.0668420i$	$-0.0286191 - 0.0304143i$	$0.00785932 + 0.0155636i$
$n = 1$	$-0.537460 + 1.242920i$	$0.208289 - 0.324589i$	$-0.122114 + 0.111058i$	$0.0768867 - 0.0372097i$
$n = 2$	$1.27404 + 0.144452i$	$-0.517466 - 0.210031i$	$0.246188 + 0.206043i$	$-0.109831 - 0.176008i$
$n = 3$	$-0.507006 - 0.739057i$	$0.0267961 + 0.540228i$	$0.156039 - 0.382678i$	$-0.232685 + 0.239092i$

TABLE IV. Rescaled excitation coefficients  $\tilde{C}_q$  for  $l = 2, 3, 4, 5$  for particle with energy  $E = 1$  (top) and  $E = 10$  (bottom).

In order to compute the time-domain waveform generated by an infalling particle, we first work in the frequency domain. For a fixed (real) frequency  $\omega$ , we integrate the homogeneous Zerilli equation using a fourth-order accurate Runge-Kutta integrator. We use the boundary condition that  $\Psi^{(+)} \sim e^{-i\omega r_*}$  close to the horizon and we integrate the homogeneous equation outwards up to some large value of  $r$ . Starting from the numerically constructed homogeneous solutions, we can use a Green's function technique to find the solution of the inhomogeneous equation [48, 50, 52]. Finally, we perform an inverse Fourier transform to compute the time-domain wave function.

### C. Regularization at the horizon

In order to find the excitation factors, one needs to evaluate Eq. (62) at the complex QNM frequency. At the horizon ( $r \rightarrow 1$ ) the integrand appearing in the quantity  $I_q^{(+)}$ , as defined in Eq. (63), can be written as a Frobenius series of the form

$$e^{i\omega_q r_*} \psi_q^{(+)}(r) q^{(+)}(r, \omega_q) = \sum_{n=0}^{\infty} \xi_n (r-1)^{\zeta_q+n}. \quad (67)$$

The convergent or divergent nature of the integral depends on the value of  $\zeta_q$ , which in turn is determined by

the behavior of the source term  $q(r, \omega_q)$  as  $r \rightarrow 1$ . Since the wave function  $\psi_q^{(+)}(r) \sim (r-1)^{-2i\omega_q}$  as  $r \rightarrow 1$ , the source term (64) diverges as  $(r-1)^{1-i\omega_q}$  at the horizon. Therefore  $\zeta_q = -2i\omega_q$  and the integral is, in general, divergent. The divergence can be regularized following the method proposed by Detweiler and Szedenits [53]. The idea is to add to the integrand a total derivative which vanishes at the horizon:

$$f(r) \equiv \frac{d}{dr} \left( \sum_{n=0}^N b_n \frac{(r-1)^{\zeta_q+n+1}}{\zeta_q+n+1} e^{-(r-1)} \right), \quad (68)$$

where  $N$  is greater than (or equal to) the largest integer in the real part of  $-2i\omega_q$ . For Schwarzschild infalls, the coefficients  $b_n$  in this expansion can be determined order-by-order in terms of the  $\xi_n$ . The first few coefficients are listed in Appendix A 1, and the values of the ‘‘excitation integrals’’  $\tilde{I}_q$  are listed in Table III.

The values of the corresponding excitation coefficients  $\tilde{C}_q = B_q^{(+)} \tilde{I}_q$  are listed in Table IV. These tables were produced using a constant value  $N = 2$  in Eq. (68), which is sufficient to regularize the divergence for the first few overtones ( $n = 0, 1, 2, 3$ ). We verified that our results are insensitive to variations of  $N$  within at least six digits, as long as  $N$  is large enough to eliminate the divergence.

The tables show some interesting trends. For example, if we consider infalls from rest ( $E = 1$ ) and a fixed multipolar index  $l$ , we see that the real part of the excitation

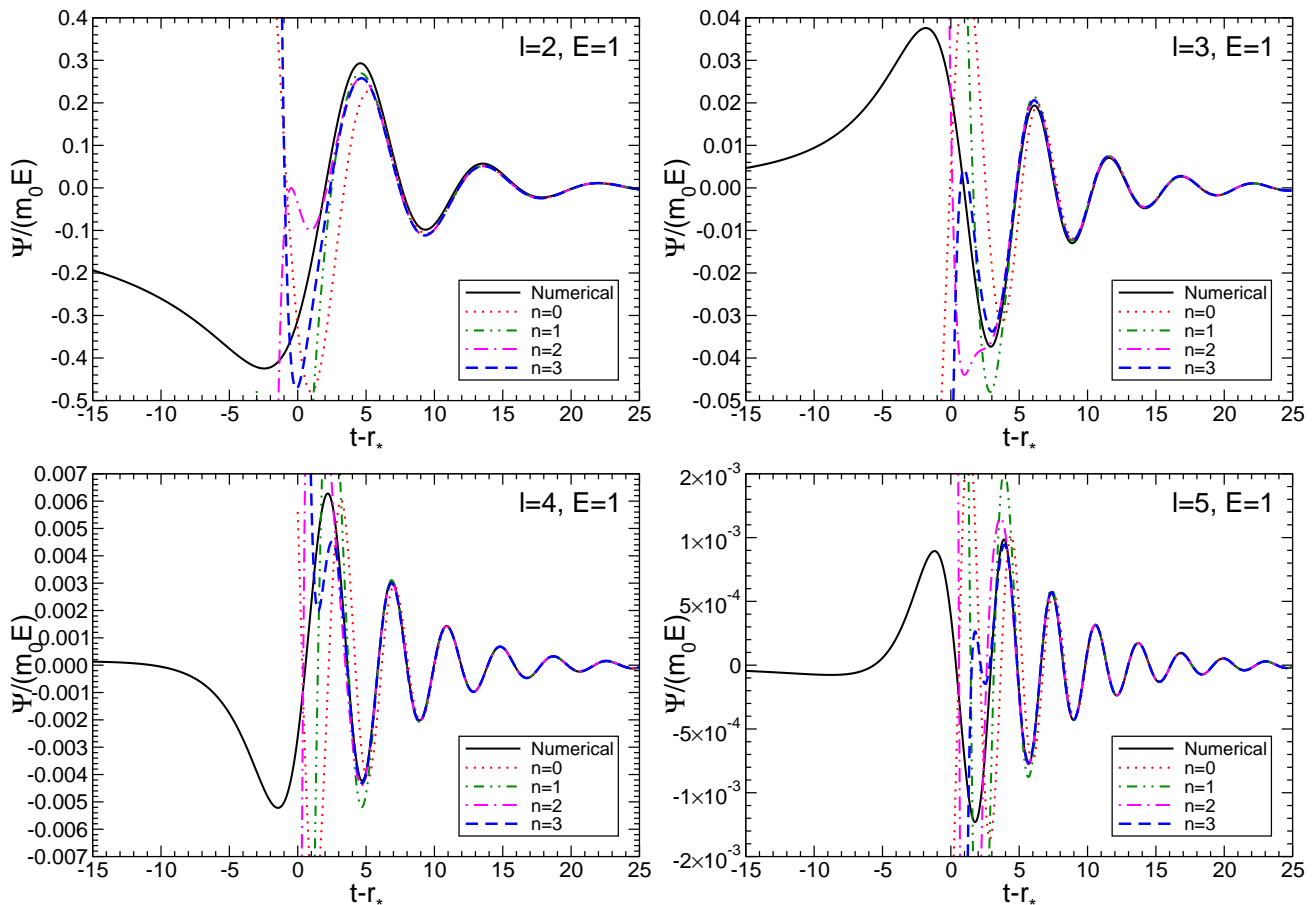


FIG. 1. Different multipolar components of the radiation ( $l = 2, 3, 4, 5$ ) for an infall from rest. Solid black lines are obtained from a numerical solution of the perturbation equations in the Fourier domain [13, 50], followed by an inverse Fourier transform. The other lines are obtained by summing an increasing numbers of overtones in the excitation coefficient calculation, as indicated in the legend. In this plot, as everywhere else in the paper, we use units  $2M = 1$ .

integral  $\tilde{I}_q$  increases as a function of the overtone index  $n$ . However this increase is compensated by a comparable decrease in the imaginary part of  $\tilde{I}_q$ , so that  $|\tilde{I}_q|$  is roughly constant as a function of  $n$ .

Figure 1 compares the excitation coefficient calculation of Eq. (8) against numerical gravitational waveforms for particles falling radially from rest. These waveforms were computed using the frequency-domain codes described in [13, 50], and then Fourier-transformed back in time. Each panel corresponds to a fixed multipole index ( $l = 2, 3, 4, 5$ ), and different line styles correspond to ringdown waveforms obtained summing a different number of overtones. This plot generalizes and extends a similar comparison that can be found in Fig. 10 of Leaver’s original paper [1]. Leaver found a disagreement at the 10% level, that he attributed to inaccuracies in the Fourier transform of the numerical waveforms. We have similar accuracy problems with the Fourier transform of our data (computing Fourier amplitudes at low frequencies  $\omega$  is time consuming, because the computational domain must extend out to a radius  $r \sim 1/\omega$ ), but

the level of disagreement that we observe is smaller than in Leaver’s original analysis. Furthermore, the agreement between our numerics and the excitation coefficient calculation gets better as  $l$  grows. Figure 1 shows quite clearly that the addition of higher overtones generally improves the agreement between the excitation coefficient calculation and the full numerical waveform at early times. However there is no analytical proof that the expansion in terms of overtones should be convergent [1], and indeed in a few isolated cases an expansion including a large number of overtones can perform more poorly than a similar expansion including a smaller number of overtones.

Figure 2 is similar to Figure 1, but it refers to a relativistic infall with (normalized) particle energy  $E = 10$ . This figure shows that even by adding four overtones we don’t get excellent agreement at the “absolute maximum” of the numerical waveform. Part of the reason is that we can only get accurate numerical amplitudes at frequencies  $M\omega \gtrsim 10^{-3}$ : to remove “memory effects” in the inverse Fourier transform, we extrapolate our numer-

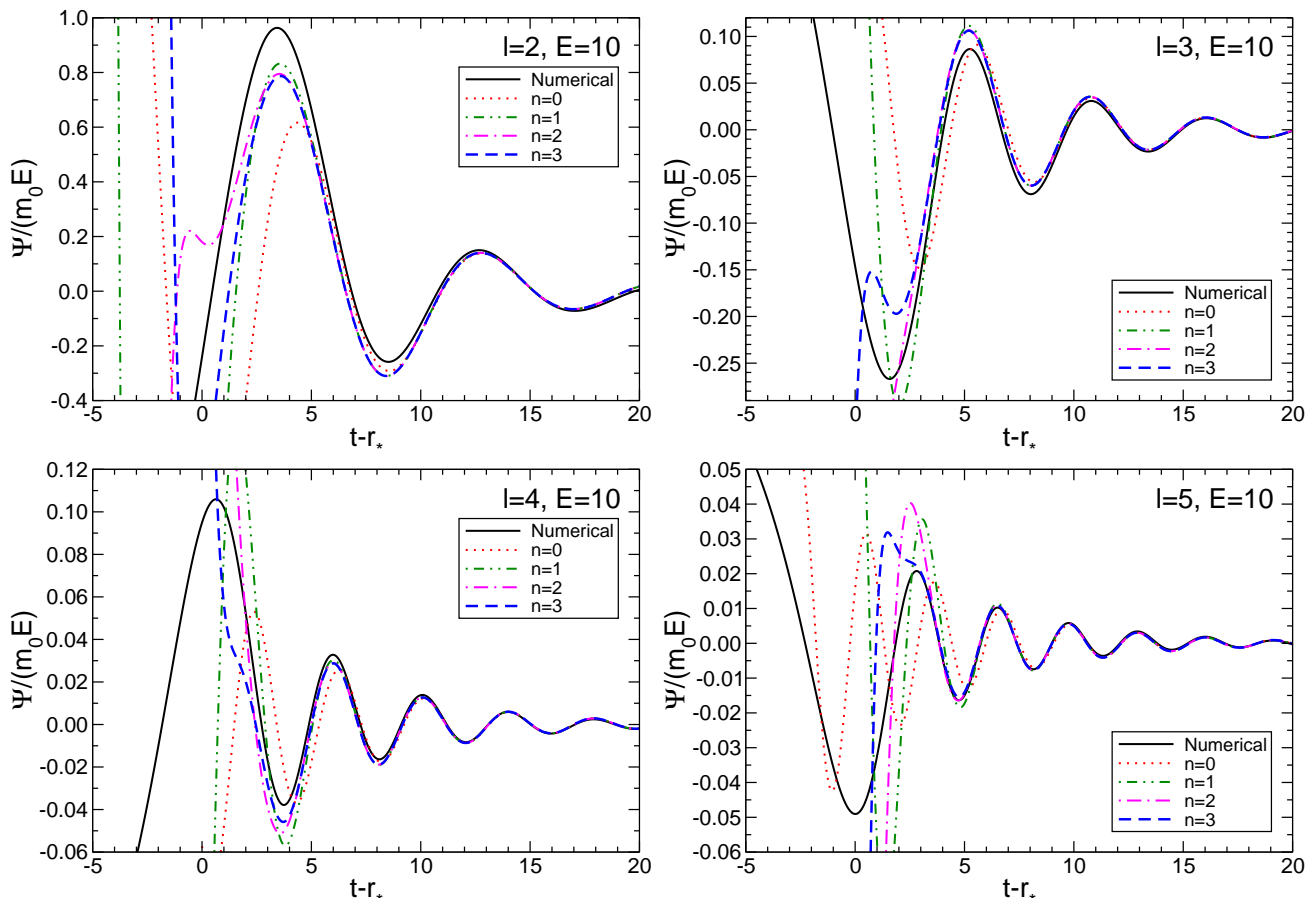


FIG. 2. Different multipolar components of the radiation ( $l = 2, 3, 4, 5$ ) for an infall with initial energy  $E = 10$ . Solid black lines are results from the numerical solution of the perturbation equations; the other lines are results obtained by summing different numbers of overtones. In this plot, as everywhere else in the paper, we use units  $2M = 1$ .

ical calculations to obtain the Fourier-domain waveform amplitude at frequencies  $M\omega \lesssim 10^{-3}$ . More importantly, in ultrarelativistic infalls a larger fraction of the energy is radiated during the infall (at low frequencies) than in the case of infalls from rest. In other words, a larger fraction of the radiation is produced *before* the beginning of the ringdown phase, and this explains the larger disagreement between numerical waveforms and “pure ringdown” waveforms. As in the nonrelativistic case, we observe that: (i) the ringdown waveform agrees better with the numerical solution as  $l$  grows; (ii) the addition of higher overtones improves the agreement between the excitation coefficient expansion and the numerical waveforms, but to a lesser extent, for the reasons explained above.

#### IV. EXCITATION FACTORS AND EXCITATION COEFFICIENTS FOR KERR BLACK HOLES

In this section we extend our calculation to particles falling into Kerr BHs. For simplicity, we consider a particle falling ultrarelativistically along the symmetry axis.

In this case the source term of the Sasaki-Nakamura equation (41) simplifies considerably [48, 52]:

$$\mathcal{S} = -\frac{m_0 E C_l^a \gamma \Delta}{2\omega^2 r^2 (r^2 + a^2)^{3/2}} e^{-i\omega r_*}, \quad (69)$$

where

$$C_l^a = \lim_{\theta \rightarrow 0} \frac{8S_{l0\omega}(\theta, \phi)}{\sin^2 \theta}, \quad (70)$$

and  $\gamma$  was defined in (43). The constants  $C_l^a$  were determined by solving the angular eigenvalue problem through a continued fraction representation, and then plugging these eigenvalues into the series solution providing the spheroidal wave functions  $S_{l0\omega}$  [5, 27]. The procedure to determine the time-domain solution of the Sasaki-Nakamura wave function  $X$  is identical to that adopted for the Schwarzschild case: i.e., first we solve the equations in the frequency domain, and then we Fourier transform back in time, applying a low-frequency extrapolation when this is necessary to remove memory effects.

Figure 3 (which is similar to Figure 1) compares the excitation coefficient calculation of Eq. (8) – where now

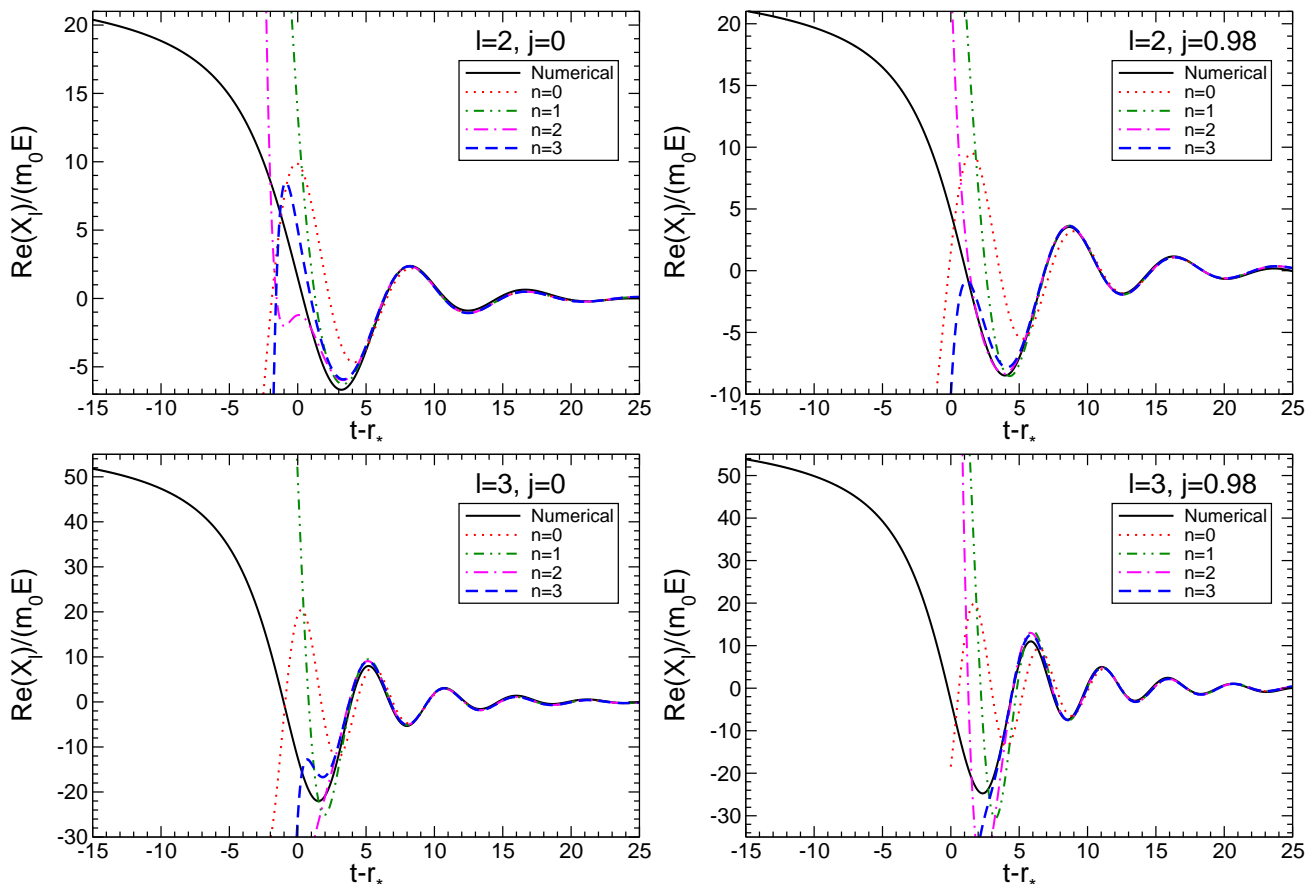


FIG. 3. Sasaki-Nakamura wave function for an ultrarelativistic infall along the symmetry axis of a Kerr BH. Solid black lines are results from the numerical solution of the perturbation equations; the other lines are results obtained by summing different numbers of overtones. The upper panels refer to  $l = 2$ , the lower panels to  $l = 3$ . The left panels corresponds to the Schwarzschild limit ( $j = 0$ ), and the right panels to a fast-spinning Kerr BH with  $a = 0.49$  ( $j = 0.98$ ). In this plot, as everywhere else in the paper, we use units  $2M = 1$ .

$\Psi$  must be understood as the Sasaki-Nakamura wave function – against numerical gravitational waveforms obtained in this way. As in the Schwarzschild case, the integrand appearing in the calculation of the Kerr excitation factors is, in general, divergent. The divergence can be regularized following a procedure analogous to the Schwarzschild case (cf. Appendix A 2).

Figure 3 confirms our basic findings from the nonrotating case: the convergence of the QNM expansion is not necessarily monotonic, and the excitation coefficient expansion works better for higher values of  $l$ . Notice that a relatively small number of overtones is sufficient to reproduce the numerical waveform at early times even when the spin of the Kerr BH is rather large ( $j = 0.98$ ), so that one may in principle expect that a larger number of overtones would be necessary (see e.g. [29, 54–57]). To our knowledge, the calculation presented in this Section is the first concrete proof that an excitation-coefficient expansion is applicable and useful in the Kerr case: all calculations available in the literature so far were specific to the Schwarzschild case (see e.g. [32, 33]).

## V. CONCLUSIONS AND OUTLOOK

In this paper we have implemented a new method, based on the MST formalism, to compute the excitation factors  $B_q$  for Kerr QNMs. This method is simpler and more accurate than the method used by two of us in [2], allowing us to extend the calculation to higher angular multipoles  $l$  and to higher overtone numbers  $n$ . Tables of the excitation factors  $B_q$  in the Teukolsky and Sasaki-Nakamura formalisms will be made publicly available online [39], in the hope to stimulate further research in this field.

As a test of the method, we have computed the QNM excitation coefficients for the classic problem of particles falling radially into the BH. We have compared the excitation coefficient expansion against numerical results for: (i) particles falling from rest ( $E = 1$ ) into a Schwarzschild BH, (ii) large-energy particles ( $E = 10$ ) falling into a Schwarzschild BH, and (iii) ultrarelativistic particles falling into a Kerr BH along the symmetry axis. In all cases we found excellent agreement, validating the useful-

ness of excitation coefficient calculations in the analytical modeling of the ringdown phase.

In order of increasing complexity, extensions of this work could consider (i) particles falling with arbitrary energy along the  $z$ -axis of a Kerr BH, (ii) particles with arbitrary energies plunging into Kerr BHs along equatorial orbits, (iii) generic orbits in Schwarzschild or Kerr, and (iv) possible applications of these calculations to the construction of semianalytical waveform templates for comparable-mass mergers. We believe that these extensions are crucial for a better understanding of the ringdown phase and (more ambitiously) for the construction of gravitational-wave detection templates for comparable-mass BH binaries.

## VI. ACKNOWLEDGMENTS

We are grateful to Sam Dolan for correspondence on the calculation of the excitation factors. E.B. and Z.Z.'s research was supported by NSF Grant No. PHY-0900735 and NSF CAREER Grant No. PHY-1055103. V.C. acknowledges partial financial support provided under the European Union's FP7 ERC Starting Grant "The dynamics of black holes: testing the limits of Einstein's theory" grant agreement no. DyBHo-256667, the NRHEP 295189 FP7-PEOPLE-2011-IRSES Grant, and FCT-Portugal through project CERN/FP/123593/2011. Research at Perimeter Institute is supported by the Government of Canada through Industry Canada and by the

Province of Ontario through the Ministry of Economic Development and Innovation.

## Appendix A: Regularization coefficients

### 1. The Schwarzschild case

For reference, in this Appendix we list the first few regularization coefficients  $b_n$  defined in Eq. (68):

$$\begin{aligned} b_0 &= \xi_0, \\ b_1 &= \xi_1 + \frac{2 - 2i\omega_q}{1 - 2i\omega_q} b_0, \\ b_2 &= \xi_2 + \frac{2i\omega_q - 3}{2(1 - 2i\omega_q)} b_0 + \frac{3 - 2i\omega_q}{2(1 - i\omega_q)} b_1, \\ b_3 &= \xi_3 + \frac{2 - i\omega_q}{3(1 - 2i\omega_q)} b_0 + \frac{i\omega_q - 2}{2(1 - i\omega_q)} b_1 + \frac{2(2 - i\omega_q)}{3 - 2i\omega_q} b_2, \\ b_4 &= \xi_4 + \frac{2i\omega_q - 5}{24(1 - 2i\omega_q)} b_0 + \frac{5 - 2i\omega_q}{12(1 - i\omega_q)} b_1 \\ &\quad + \frac{2i\omega_q - 5}{2(3 - 2i\omega_q)} b_2 + \frac{5 - 2i\omega_q}{2(2 - i\omega_q)} b_3. \end{aligned} \tag{A1}$$

### 2. The Kerr case

The regularization coefficients for the Kerr case are much more lengthy than in the nonrotating case, but their calculation is straightforward. Here we list for reference the first two coefficients:

$$\begin{aligned} b_0 &= \frac{1}{A_{\text{out}} \omega_q^2 r_+^2} (r_+ - r_-) \left( \frac{2i\omega_q r_+}{r_+ - r_-} - 1 \right) (ir_+ - ir_- + \omega_q r_+) (2ir_+ - i + 2\omega_q r_+), \\ b_1 &= 2b_0 \frac{r_- - r_+ + i\omega_q r_+}{r_- - r_+ + 2i\omega_q r_+} + \frac{1}{2A_{\text{out}}^{\text{SN}} \omega_q^2 r_+^3} (r_+ - r_-) \frac{3r_+ - 3r_- - 2i\omega_q r_+}{r_- - r_+} \\ &\quad \times \left\{ r_-^4 (8 + 4ir_+ \omega_q) + r_-^3 \left[ 4 + r_+ (-36 + \lambda + 12i\omega_q) - 2r_+^2 \omega_q (5i + 2\omega_q) \right] \right. \\ &\quad + r_-^2 r_+ \left[ -11 + 4i\omega_q + 6r_+^2 \omega_q (i + 2\omega_q) + 3a_{r_1} - r_+ (-58 + 3\lambda + 38i\omega_q + 4\omega_q^2 + 6a_{r_1} - 6i\omega_q a_{r_1}) \right] \\ &\quad + r_+^3 \left[ 4\omega_q^2 + 2r_+^2 \omega_q (-i + 2\omega_q) - 2i\omega_q (-5 + a_{r_1}) + 3(-1 + a_{r_1}) - r_+ \left( \lambda + 2(1 - i\omega_q) (-5 + 4\omega_q^2 - 2i\omega_q (-4 + a_{r_1}) + 3a_{r_1}) \right) \right] \\ &\quad \left. + r_- r_+^2 \left[ 2r_+^2 (i - 6\omega_q) \omega_q + 2(5 + i\omega_q (-7 + a_{r_1}) - 3a_{r_1}) + r_+ \left( 3\lambda - 4(10 + \omega_q^2 (-5 + a_{r_1}) - 3a_{r_1} + i\omega_q (-13 + 4a_{r_1})) \right) \right] \right\}, \end{aligned} \tag{A2}$$

where

$$\sigma_+ = \frac{\omega_q r_+ - am}{r_+ - r_-}, \tag{A3}$$

the amplitude  $A_{\text{out}}^{\text{SN}}$  is related to the Teukolsky amplitude  $A_{\text{out}}^{\text{T}} = \sum_{n=0}^{\infty} a_{rn}$  via Eq. (47) and  $\lambda$  is related to

the separation constant  $A_{lm}$  through relation (20). The coefficients  $\{a_{rn}\}$ ,  $n = 0, 1, 2, \dots$  (with  $a_{r0} = 1$ ) are defined via the homogeneous solution  $R_{r_+}$  of the Teukolsky equation



$$R_{r_+} = e^{i\omega_q r} (r - r_-)^{-1-s+i\omega_q+i\sigma_+} (r - r_+)^{-s-i\sigma_+} \sum_{n=0}^{\infty} a_{rn} \left( \frac{r - r_+}{r - r_-} \right)^n, \quad (\text{A4})$$

and can be obtained by plugging this decomposition in the Teukolsky equation (10).

The Sasaki-Nakamura wave function  $X$  is related to  $R_{r_+}$  by Eq. (38). What we plot in Figure 3 is actually the normalized Sasaki-Nakamura wave form  $X_q^{\text{SN}} = (X e^{-i\omega_q r_*})/A_{\text{out}}$ , whose excitation coefficients are given by

$$C_q = -\gamma_{\infty} \int_{r_+}^{\infty} dr \left[ \frac{X_q^{\text{SN}}}{2\omega_q^2 r^2 \sqrt{(r - r_+)(r - r_-) + r}} - \sum_{k=0}^{\infty} \left( e^{-r+r_+} (r - r_+)^{k + \frac{2i\omega_q r_+}{r_- - r_+}} b_k - \frac{e^{-r+r_+} (r - r_+)^{1+k + \frac{2i\omega_q r_+}{r_- - r_+}}}{1 + k + \frac{2i\omega_q r_+}{r_- - r_+}} b_k \right) \right].$$

- [1] E. W. Leaver, Phys. Rev. **D34**, 384 (1986).  
[2] E. Berti and V. Cardoso, Phys. Rev. **D74**, 104020 (2006), arXiv:gr-qc/0605118.  
[3] K. D. Kokkotas and B. G. Schmidt, Living Rev. Relativity **2** (1999), arXiv:gr-qc/9909058.  
[4] H.-P. Nollert, Class. Quantum Grav. **16**, R159 (1999).  
[5] E. Berti, V. Cardoso, and A. O. Starinets, Class. Quantum Grav. **26**, 163001 (2009), arXiv:0905.2975 [gr-qc].  
[6] F. Pretorius, “Binary Black Hole Coalescence,” in *Physics of relativistic objects in compact binaries: from birth to coalescence (Astrophysics and Space Science Library, Vol. 359)* (Springer, New York, 2007) Chap. 9, arXiv:0710.1338 [gr-qc].  
[7] U. Sperhake, E. Berti, and V. Cardoso, (2011), arXiv:1107.2819 [gr-qc].  
[8] H. P. Pfeiffer, Class.Quant.Grav. **29**, 124004 (2012), arXiv:1203.5166 [gr-qc].  
[9] U. Sperhake, (2013), arXiv:1301.3772 [gr-qc].  
[10] J. A. González, U. Sperhake, and B. Brügmann, Phys. Rev. **D79**, 124006 (2009), arXiv:0811.3952 [gr-qc].  
[11] C. O. Lousto, H. Nakano, Y. Zlochower, and M. Campanelli, Phys. Rev. **D82**, 104057 (2010), arXiv:1008.4360 [gr-qc].  
[12] H. Nakano, Y. Zlochower, C. O. Lousto, and M. Campanelli, Phys. Rev. **D84**, 124006 (2011), arXiv:1108.4421 [gr-qc].  
[13] U. Sperhake, V. Cardoso, C. D. Ott, E. Schnetter, and H. Witek, Phys.Rev. **D84**, 084038 (2011), arXiv:1105.5391 [gr-qc].  
[14] W. E. East and F. Pretorius, (2013), arXiv:1303.1540 [gr-qc].  
[15] C. O. Lousto, H. Nakano, Y. Zlochower, B. C. Mundim, and M. Campanelli, Phys.Rev. **D85**, 124013 (2012), arXiv:1203.3223 [gr-qc].  
[16] G. Lovelace, R. Owen, H. P. Pfeiffer, and T. Chu, Phys.Rev. **D78**, 084017 (2008), arXiv:0805.4192 [gr-qc].  
[17] G. Lovelace, M. Scheel, and B. Szilagyi, Phys.Rev. **D83**, 024010 (2011), arXiv:1010.2777 [gr-qc].  
[18] G. Lovelace, M. Boyle, M. A. Scheel, and B. Szilagyi, Class. Quantum Grav. **29**, 045003 (2012), arXiv:1110.2229 [gr-qc].  
[19] A. Taracchini, Y. Pan, A. Buonanno, E. Barausse, M. Boyle, *et al.*, Phys.Rev. **D86**, 024011 (2012), arXiv:1202.0790 [gr-qc].  
[20] E. Berti, M. Cavaglià, and L. Gualtieri, Phys. Rev. **D69**, 124011 (2004), arXiv:hep-th/0309203.  
[21] E. Berti, V. Cardoso, and B. Kipapa, Phys. Rev. **D83**, 084018 (2011), arXiv:1010.3874 [gr-qc].  
[22] H. Witek, V. Cardoso, L. Gualtieri, C. Herdeiro, U. Sperhake, and M. Zilhão, Phys. Rev. **D83**, 044017 (2011), arXiv:1011.0742 [gr-qc].  
[23] H. M. S. Yoshino and M. Shibata, Prog.Theor.Phys.Suppl. **189**, 269 (2011).  
[24] V. Cardoso, L. Gualtieri, C. Herdeiro, U. Sperhake, P. M. Chesler, *et al.*, Class.Quant.Grav. **29**, 244001 (2012), arXiv:1201.5118 [hep-th].  
[25] S. A. Teukolsky, Phys. Rev. Lett. **29**, 1114 (1972).  
[26] S. A. Teukolsky, Astrophys. J. **185**, 635 (1973).  
[27] E. Berti, V. Cardoso, and M. Casals, Phys. Rev. **D73**, 024013 (2006), arXiv:gr-qc/0511111.  
[28] H.-P. Nollert and R. H. Price, J. Math. Phys. **40**, 980 (1999), arXiv:gr-qc/9810074.  
[29] E. Berti, V. Cardoso, and C. M. Will, AIP Conf. Proc. **848**, 687 (2006), arXiv:gr-qc/0601077.  
[30] E. N. Dorband, E. Berti, P. Diener, E. Schnetter, and M. Tiglio, Phys. Rev. **D74**, 084028 (2006), arXiv:gr-qc/0608091.  
[31] Y. Sun and R. H. Price, Phys. Rev. **D38**, 1040 (1988).  
[32] S. Hadar and B. Kol, Phys. Rev. **D84**, 044019 (2011), arXiv:0911.3899 [gr-qc].  
[33] S. Hadar, B. Kol, E. Berti, and V. Cardoso, Phys. Rev. **D84**, 047501 (2011), arXiv:1105.3861 [gr-qc].  
[34] M. Sasaki and T. Nakamura, Prog. Theor. Phys. **67**, 1788 (1982).  
[35] T. Regge and J. A. Wheeler, Phys. Rev. **108**, 1063 (1957).  
[36] F. J. Zerilli, Phys. Rev. **D2**, 2141 (1970).  
[37] S. Mano, H. Suzuki, and E. Takasugi, Prog. Theor. Phys. **95**, 1079 (1996), arXiv:gr-qc/9603020.  
[38] S. Mano, H. Suzuki, and E. Takasugi, Prog. Theor. Phys. **96**, 549 (1996), arXiv:gr-qc/9605057.

- [39] Webpage with Mathematica notebooks and numerical quasinormal mode Tables:  
<http://www.phy.olemiss.edu/~berti/qnms.html>  
<http://gamow.ist.utl.pt/~vitor/ringdown.html>.
- [40] S. Mano and E. Takasugi, *Prog. Theor. Phys.* **97**, 213 (1997), arXiv:gr-qc/9611014.
- [41] E. W. Leaver, *Proc. R. Soc. London, Ser. A* **402**, 285 (1985).
- [42] M. Sasaki and H. Tagoshi, *Living Rev. Relativity* **6** (2003), arXiv:gr-qc/0306120.
- [43] S. Chandrasekhar, *The Mathematical Theory of Black Holes* (Clarendon Press, Oxford, U.K., 1983).
- [44] M. Davis, R. J. Ruffini, W. H. Press, and R. H. Price, *Phys. Rev. Lett.* **27**, 1466 (1971).
- [45] V. Ferrari and R. Ruffini, *Phys. Lett.* **B98**, 381 (1981).
- [46] C. O. Lousto and R. H. Price, *Phys. Rev.* **D55**, 2124 (1997), arXiv:gr-qc/9609012.
- [47] V. Cardoso and J. P. S. Lemos, *Phys. Lett.* **B538**, 1 (2002), arXiv:gr-qc/0202019.
- [48] V. Cardoso and J. P. S. Lemos, *Gen. Rel. Grav.* **35**, 327 (2003), arXiv:gr-qc/0207009.
- [49] H. Kodama and A. Ishibashi, *Prog. Theor. Phys.* **110**, 701 (2003), arXiv:hep-th/0305147.
- [50] E. Berti, V. Cardoso, T. Hinderer, M. Lemos, F. Pretorius, U. Sperhake, and N. Yunes, *Phys. Rev.* **D81**, 104048 (2010), arXiv:1003.0812 [gr-qc].
- [51] E. Mitsou, *Phys. Rev.* **D83**, 044039 (2011), arXiv:1012.2028 [gr-qc].
- [52] V. Cardoso and J. P. S. Lemos, *Phys. Rev.* **D67**, 084005 (2003), arXiv:gr-qc/0211094.
- [53] S. L. Detweiler and J. Szedenits, Eugene, *Astrophys. J.* **231**, 211 (1979).
- [54] N. Andersson and K. Glampedakis, *Phys. Rev. Lett.* **84**, 4537 (2000), arXiv:gr-qc/9909050 [gr-qc].
- [55] V. Cardoso, *Phys. Rev.* **D70**, 127502 (2004), arXiv:gr-qc/0411048.
- [56] E. Berti, V. Cardoso, and C. M. Will, *Phys. Rev.* **D73**, 064030 (2006), arXiv:gr-qc/0512160.
- [57] H. Yang, F. Zhang, A. Zimmerman, D. A. Nichols, E. Berti, *et al.*, *Phys. Rev.* **D87**, 041502 (2013), arXiv:1212.3271 [gr-qc].